The Aberrance of the 4*S* Diastereomer of 4-Hydroxyproline

Matthew D. Shoulders, Frank W. Kotch, Amit Choudhary, Ilia A. Guzei, and Ronald T. Raines*

Sedimentation Equilibrium Experiments on $(hypProGly)_{15}$, $(mopProGly)_{15}$, and $(ProProGly)_{15}$. Sedimentation equilibrium experiments were performed with a Beckman XL-A Analytical Ultracentrifuge at the University of Wisconsin Biophysics Instrumentation Facility. Samples were diluted to approximately 0.1 mM in 50 mM potassium phosphate buffer (pH 3) and equilibrated at ≤4 °C for ≥24 h. Equilibrium data were collected at multiple speeds at both 4 and 40 °C. Gradients were monitored at 230 nm. Solvent densities of 1.0048 and 0.99699 g/mL at 4 and 40 °C, respectively, were calculated based on buffer composition and temperature. Partial specific volumes ($\bar{\nu}$) for $(hypProGly)_{15}$, $(mopProGly)_{15}$, and $(ProProGly)_{15}$ were calculated based on amino acid content, with corrections for hydroxyl or methoxy content.[1] Values of $\bar{\nu}$ = 0.694, 0.728, and 0.729 cm^3/g were used for $(hypProGly)_{15}$, $(mopProGly)_{15}$, and $(ProProGly)_{15}$, respectively. Data were analyzed with programs written for IgorPro (Wavemetrics) by Dr. Darrell R. McCaslin (Univeristy of Wisconsin–Madison).

A log plot of absorbance versus the square of the distance from the center of rotation is shown in Figure S1. The slope at any point is proportional to the weight-averaged molecular weight, provided that the extinction coefficients per unit mass of assembled and monomeric peptides are equivalent.

Sedimentation equilibrium results at 40 °C are consistent with a single monomeric species for $(hypProGly)_{15}$, a mixture of primarily monomer and some trimer for $(mopProGly)_{15}$, and a mixture of primarily trimer and some monomer for $(ProProGly)_{15}$, as shown in Figure S1. At 4 °C, the dramatic change in gradient for $(hypProGly)_{15}$ and $(mopProGly)_{15}$ is consistent with the assembly of these species into a triple helix. The fit shown at 4 °C for these two peptides (Figure S1) is based on a mixture of primarily trimer and some monomer. The data at 4 °C for $(ProProGly)_{15}$ also indicates assembly for this peptide at low temperature, but the change in gradient is smaller for $(ProProGly)_{15}$ because it remains largely assembled even at 40 °C. The fit shown in Figure S2 for $(ProProGly)_{15}$ at 4 °C is for a mixture of primarily trimer and some monomer.

Structure Determination of Ac-hyp-OMe. The crystals of Ac-hyp-OMe used for X-ray structure determination were obtained by dissolving the white solid in a minimum of EtOAc, equilibrating with a reservoir of hexanes, and allowing the solvent to slowly evaporate over ~2 weeks. A colorless crystal with approximate dimensions 0.44 mm × 0.11 mm × 0.10 mm was selected under oil under ambient conditions and attached to the tip of a MiTeGen MicroMount©. The crystal was mounted in a stream of cold nitrogen at 100(2) K and centered in the X-ray beam by using a video camera. The crystal evaluation and data collection were performed on a Bruker SMART APEXII diffractometer with Cu K_α (λ = 1.54178 Å) radiation and the diffractometer to crystal distance of 4.03 cm.

The initial cell constants were obtained from three series of ω scans at different starting angles. Each series consisted of 50 frames collected at intervals of 0.5° in a 25° range about ω with the exposure time of 60 s per frame. The reflections were successfully indexed by an automated indexing routine built in the SMART program. The final cell constants were calculated from a set of 2361 strong reflections from the actual data collection.

The data were collected by using the full sphere data collection routine to survey the reciprocal space to the extent of a full sphere to a resolution of 0.82 Å. A total of 9359 data were harvested by collecting 14 sets of frames with 0.5° scans in ω with an exposure time 15–30 s per frame. These highly redundant datasets were corrected for Lorentz and polarization effects. The absorption correction was based on fitting a function to the empirical transmission surface as sampled by multiple equivalent measurements.[2]

The systematic absences in the diffraction data were uniquely consistent for the space groups $P2_12_12_1$ that yielded chemically reasonable and computationally stable results of refinement.[3] A successful solution by the direct methods provided most non-hydrogen atoms from the *E*-map. The remaining non-hydrogen atoms were located in an alternating series of least-squares cycles and difference Fourier maps. All non-hydrogen atoms were refined with anisotropic displacement coefficients. All hydrogen atoms were included in the structure factor calculation at idealized positions and were allowed to ride on the neighboring atoms with relative isotropic displacement coefficients.

The best crystal selected for a single-crystal X-ray diffraction experiment proved to be a split crystal with approximately a 4:1 contribution ratio between the two components. The final refinement presented here is based on the major component only. The absolute configuration of the compound could not be established unambiguously from crystallography, but is known to be 2*S*,4*S* from the synthetic route. The final least-squares refinement of 121 parameters against 984 data resulted in residuals *R* (based on F^2 for $I \geq 2\sigma$) and *wR* (based on F^2 for all data) of 0.0381 and 0.1022, respectively. The final difference Fourier map was featureless. Data related to the structure of Ac-hyp-OMe are presented in Tables S3–S8.

Structure Determination of Boc-mop-OH (8). The crystals of Boc-mop-OH (**8**) suitable for X-ray analysis were obtained by dissolving the compound in a minimum of $CDCl_3$ and allowing the solvent to slowly evaporate over ~2 weeks. A colorless crystal with approximate dimensions 0.52 mm × 0.36 mm × 0.10 mm was selected under oil under ambient conditions and attached to the tip of a Micromount©. The crystal was mounted in a stream of cold nitrogen at 100(2) K and centered in the X-ray beam by using a video camera. The crystal evaluation and data collection were performed on a Bruker CCD-1000 diffractometer with Mo K_α (λ = 0.71073 Å) radiation and the diffractometer to crystal distance of 4.9 cm.

The initial cell constants were obtained from three series of ω scans at different starting angles. Each series consisted of 60 frames collected at intervals of 0.3° in a 6° range about ω with the exposure time of 15 s per frame. The reflections were successfully indexed by an automated indexing routine built in the SMART program. The final cell constants were calculated from a set of 6766 strong reflections from the actual data collection.

The data were collected by using the full-sphere data collection routine to survey the reciprocal space to the extent of a full sphere to a resolution of 0.80 Å. A total of 20594 data were harvested by collecting four sets of frames with 0.36° scans in ω and one set with 0.45° scans in φ with an exposure time of 41 s per frame. These highly redundant datasets were corrected for Lorentz and polarization effects. The absorption correction was based on fitting a function to the empirical transmission surface as sampled by multiple equivalent measurements.[2]

The systematic absences in the diffraction data were consistent for the space group $P2_1$ that yielded chemically reasonable and computationally stable results of refinement.[2] A successful solution by the direct methods provided most non-hydrogen atoms from the *E*-map. The remaining non-hydrogen atoms were located in an alternating series of least-squares cycles and difference Fourier maps. All non-hydrogen atoms were refined with anisotropic displacement coefficients. All hydrogen atoms were included in the structure factor calculation at idealized positions and were allowed to ride on the neighboring atoms with relative isotropic displacement coefficients. The crystal is a merohedral twin with a 0.6859(17):0.3141(17) twin component ratio. The twin law is [–1 0 0 0 –1 0 0 0 1].

The final least-squares refinement of 160 parameters against 1727 data resulted in residuals *R* (based on F^2 for $I \geq 2\sigma$) and *wR* (based on F^2 for all data) of 0.0304 and 0.0771, respectively.

The final difference Fourier map was featureless. Data related to the structure of Boc-mop-OH (**8**) are presented in Tables S9–S14.

References

(1) Durschlag, H.; Zipper, P. *Prog. Colloid Polym. Sci.* **1994**, *94*, 20-39.

(2) Bruker–AXS. (2000–2003) SADABS v.2.05, SAINT v.6.22, SHELXTL v.6.10 & SMART 5.622 Software Reference Manuals. Bruker–AXS, Madison, Wisconsin.

(3) Sheldrick, G. M. *Acta Cryst.* **2008**, *A64*, 112-122.

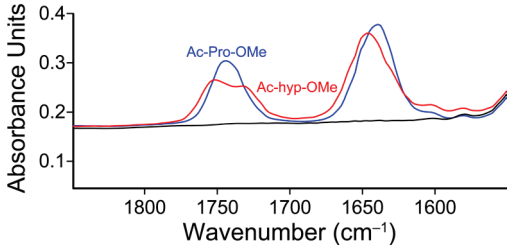

Figure S1. IR spectrum of Ac-Pro-OMe (6 mg/mL; blue) and Ac-hyp-OMe (6 mg/ml; red) in $CHCl_3$. The black line is for neat solvent. Spectra (6 scans) were acquired with a KBr cell. Ac-Pro-OMe: υ_{ester} = 1744 cm^{-1}, υ_{amide} = 1640 cm^{-1}. Ac-mop-OMe: $\upsilon_{ester,trans}$ = 1752 cm^{-1}; $\upsilon_{ester,cis}$ = 1732 cm^{-1}; υ_{amide} = 1646 cm^{-1}.

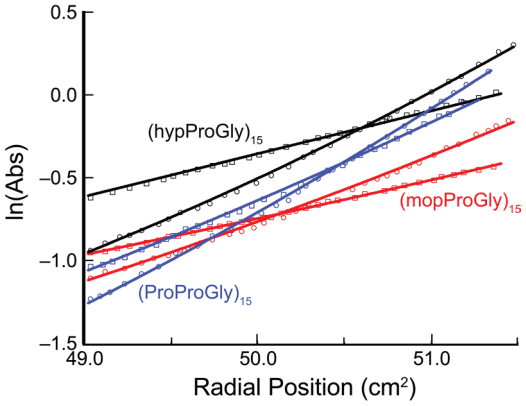

Figure S2. Sedimentation equilibrium data for $(hypProGly)_{15}$, $(mopProGly)_{15}$, and $(ProProGly)_{15}$. Data for $(hypProGly)_{10}$ (black), $(mopProGly)_{15}$ (red), and $(ProProGly)_{15}$ (blue) at a rotor speed of 34,000 rpm are displayed (for clarity, every third data point is shown). Equilibrium data were collected at 4 °C (circles) and 40 °C (squares). Gradients were monitored at 230 nm. Best fits shown are for solutions containing primarily trimer and some monomer at 4 °C for $(hypProGly)_{15}$ and $(mopProGly)_{15}$, and at 4 and 40 °C for $(ProProGly)_{15}$. Best fits shown are for solutions containing only monomer at 40 °C for $(hypProGly)_{15}$ and primarily monomer with some trimer at 40 °C for $(mopProGly)_{15}$.

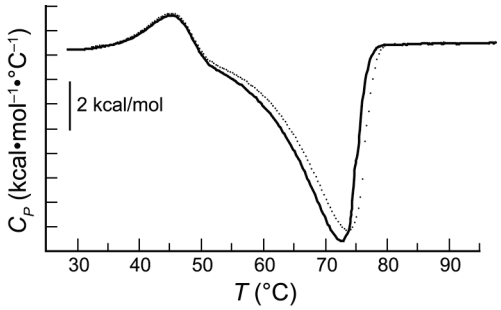

Figure S3. Raw data for DSC scans of $(mopProGly)_{15}$. The large exotherm subsequent to triple-helix denaturation is consistent with extensive aggregation at high temperatures. Thermodynamic parameters were extracted from just the first half of the endotherm, which was not affected by the putative aggregation. The initial scan is shown as a solid line. A rescan of the same sample (dotted line) after recooling shows that the transition is fully reversible.

Table S1. ^{1}H NMR Coupling Constants (J) for the trans Isomer of Ac-hyp-OMe in D_2O.

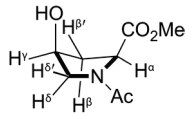

H–H	J (Hz)
H^{α}–H^{β}	9.6
H^{α}–$H^{\beta\prime}$	2.0
H^{β}–$H^{\beta\prime}$	13.8
H^{β}–H^{γ}	nd[a]
$H^{\beta\prime}$–H^{γ}	2.0
H^{β}–H^{δ}	—
$H^{\beta\prime}$–$H^{\delta\prime}$	2.0
H^{γ}–H^{δ}	4.5
H^{γ}–$H^{\delta\prime}$	2.0
H^{δ}–$H^{\delta\prime}$	11.9

[a]This coupling constant could not be determined due to overlapping peaks or higher-order effects.

Table S2. SCF Energies (atomic units; au) for Ac-hyp-OMe Calculated at the B3LYP/6-311+G(2d,p) Level of Theory.

Ac-hyp-OMe conformer	Energy	*ZPE* correction	Energy (corrected)	$E_{\text{hydrogen bond}}$[a] (kcal/mol)	$E_{n\rightarrow\pi^*}$[a] (kcal/mol)
trans, C^{γ}-endo, hydrogen bond	-668.5632064	0.214309	–668.3488974	5.95	1.00
trans, C^{γ}-endo, no hydrogen bond	-668.5554173	0.213095	–668.3423223	—	0.04
cis, C^{γ}-endo, hydrogen bond	-668.5593751	0.213953	–668.3454221	3.70	—
cis, C^{γ}-endo, no hydrogen bond	-668.555142	0.213196	–668.341946	—	—

[a]From second-order perturbation theory.

Table S3. Crystal Data and Structure Refinement for Crystalline Ac-hyp-OMe.

Identification code	raines27	
Empirical formula	$C_8H_{13}NO_4$	
Formula weight	187.19	
Temperature	100(1) K	
Wavelength	1.54178 Å	
Crystal system	Orthorhombic	
Space group	$P2_12_12_1$	
Unit cell dimensions	a = 7.5448(2) Å	α = 90°
	b = 10.5798(4) Å	β = 90°
	c = 11.1164(4) Å	γ = 90°
Volume	887.34(5) Å^3	
Z	4	
Density (calculated)	1.401 Mg/m^3	
Absorption coefficient	0.954 mm^{-1}	
F(000)	400	
Crystal size	0.44 × 0.11 × 0.10 mm^3	
Theta range for data collection	5.77–70.07°	
Index ranges	$-9 \le h \le 9$, $-12 \le k \le 12$, $-13 \le l \le 13$	
Reflections collected	1645	
Independent reflections	984 [R_{int} = 0.0275]	
Completeness to theta = 70.07°	98.4%	
Absorption correction	Empirical with SADABS	
Max. and min. transmission	0.9106 and 0.6789	
Refinement method	Full-matrix least-squares on F^2	
Data / restraints / parameters	984 / 0 / 121	
Goodness-of-fit on F^2	1.107	
Final R indices [$I > 2\sigma(I)$]	$R1$ = 0.0381, $wR2$ = 0.1003	
R indices (all data)	$R1$ = 0.0411, $wR2$ = 0.1022	
Absolute structure parameter	N/A	
Largest diff. peak and hole	0.146 and –0.224 e.Å^{-3}	

Table S4. Atomic Coordinates (10^4) and Equivalent Isotropic Displacement Parameters (Å^2 × 10^3) for Crystalline Ac-hyp-OMe.

	x	*y*	*z*	*U*(eq)[a]
O(1)	4182(2)	3473(2)	5733(2)	42(1)
O(2)	6489(2)	4809(2)	5801(2)	45(1)
O(3)	6797(2)	2766(2)	8131(2)	42(1)
O(4)	384(2)	3192(2)	8243(2)	44(1)
N(1)	3101(3)	4001(2)	7979(2)	37(1)
C(1)	4416(3)	4848(2)	7436(2)	38(1)
C(2)	5819(3)	4929(2)	8425(2)	39(1)
C(3)	5854(3)	3582(2)	8931(2)	39(1)
C(4)	3900(3)	3186(2)	8910(2)	38(1)
C(5)	1358(3)	3956(2)	7718(2)	38(1)
C(6)	681(3)	4860(2)	6782(2)	41(1)
C(7)	5173(3)	4372(2)	6258(2)	39(1)
C(8)	4777(4)	3081(3)	4556(3)	49(1)

[a] *U*(eq) is defined as one-third of the trace of the orthogonalized U^{ij} tensor.

Table S5. Bond Lengths [Å] and Angles [°] for Ac-hyp-OMe.

O(1)-C(7)	1.343(3)	C(2)-H(2A)	0.9900
O(1)-C(8)	1.444(3)	C(2)-H(2B)	0.9900
O(2)-C(7)	1.208(3)	C(3)-C(4)	1.533(3)
O(3)-C(3)	1.429(3)	C(3)-H(3B)	1.0000
O(3)-H(3A)	0.8400	C(4)-H(4A)	0.9900
O(4)-C(5)	1.238(3)	C(4)-H(4B)	0.9900
N(1)-C(5)	1.348(3)	C(5)-C(6)	1.502(3)
N(1)-C(1)	1.466(3)	C(6)-H(6A)	0.9800
N(1)-C(4)	1.476(3)	C(6)-H(6B)	0.9800
C(1)-C(7)	1.515(4)	C(6)-H(6C)	0.9800
C(1)-C(2)	1.528(3)	C(8)-H(8A)	0.9800
C(1)-H(1A)	1.0000	C(8)-H(8B)	0.9800
C(2)-C(3)	1.533(3)	C(8)-H(8C)	0.9800
C(7)-O(1)-C(8)	115.1(2)	O(1)-C(8)-H(8A)	109.5
C(3)-O(3)-H(3A)	109.5	O(1)-C(8)-H(8B)	109.5
C(5)-N(1)-C(1)	126.4(2)	H(8A)-C(8)-H(8B)	109.5
C(5)-N(1)-C(4)	121.9(2)	O(1)-C(8)-H(8C)	109.5
C(1)-N(1)-C(4)	111.68(18)	H(8A)-C(8)-H(8C)	109.5
N(1)-C(1)-C(7)	114.04(19)	H(8B)-C(8)-H(8C)	109.5
N(1)-C(1)-C(2)	101.95(19)		
C(7)-C(1)-C(2)	112.24(18)		
N(1)-C(1)-H(1A)	109.4		
C(7)-C(1)-H(1A)	109.4		
C(2)-C(1)-H(1A)	109.4		
C(1)-C(2)-C(3)	102.93(18)		
C(1)-C(2)-H(2A)	111.2		
C(3)-C(2)-H(2A)	111.2		
C(1)-C(2)-H(2B)	111.2		
C(3)-C(2)-H(2B)	111.2		
H(2A)-C(2)-H(2B)	109.1		
O(3)-C(3)-C(4)	107.71(19)		
O(3)-C(3)-C(2)	109.9(2)		
C(4)-C(3)-C(2)	103.4(2)		
O(3)-C(3)-H(3B)	111.8		
C(4)-C(3)-H(3B)	111.8		
C(2)-C(3)-H(3B)	111.8		
N(1)-C(4)-C(3)	104.1(2)		
N(1)-C(4)-H(4A)	110.9		
C(3)-C(4)-H(4A)	110.9		
N(1)-C(4)-H(4B)	110.9		
C(3)-C(4)-H(4B)	110.9		
H(4A)-C(4)-H(4B)	108.9		
O(4)-C(5)-N(1)	120.0(2)		
O(4)-C(5)-C(6)	122.7(2)		
N(1)-C(5)-C(6)	117.3(2)		
C(5)-C(6)-H(6A)	109.5		
C(5)-C(6)-H(6B)	109.5		
H(6A)-C(6)-H(6B)	109.5		
C(5)-C(6)-H(6C)	109.5		
H(6A)-C(6)-H(6C)	109.5		
H(6B)-C(6)-H(6C)	109.5		
O(2)-C(7)-O(1)	123.1(2)		
O(2)-C(7)-C(1)	123.1(2)		
O(1)-C(7)-C(1)	113.6(2)		

Table S6. Anisotropic Displacement Parameters ($Å^2 \times 10^3$) for Ac-hyp-OMe.[a]

	U^{11}	U^{22}	U^{33}	U^{23}	U^{13}	U^{11}
O(1)	32(1)	42(1)	54(1)	-4(1)	2(1)	-2(1)
O(2)	30(1)	46(1)	58(1)	2(1)	3(1)	-4(1)
O(3)	24(1)	37(1)	65(1)	-2(1)	1(1)	2(1)
O(4)	26(1)	41(1)	66(1)	3(1)	0(1)	-4(1)
N(1)	25(1)	35(1)	52(1)	2(1)	2(1)	0(1)
C(1)	24(1)	34(1)	58(1)	1(1)	1(1)	-1(1)
C(2)	25(1)	37(1)	55(1)	-1(1)	0(1)	-1(1)
C(3)	28(1)	35(1)	54(2)	-1(1)	1(1)	1(1)
C(4)	28(1)	37(1)	49(1)	2(1)	1(1)	2(1)
C(5)	26(1)	36(1)	53(1)	-5(1)	2(1)	1(1)
C(6)	27(1)	38(1)	57(1)	0(1)	-1(1)	2(1)
C(7)	26(1)	34(1)	56(1)	3(1)	-4(1)	-1(1)
C(8)	40(1)	54(2)	54(2)	-8(1)	1(1)	-2(1)

[a]The anisotropic displacement factor exponent takes the form: $-2p^2[h^2\, a^{*2}U^{11} + ... + 2\, h\, k\, a^*\, b^*\, U^{12}]$.

Table S7. Hydrogen Coordinates ($\times 10^4$) and Isotropic Displacement Parameters ($Å^2 \times 10^3$) for Ac-hyp-OMe.

	x	*y*	*z*	*U*(eq)
H(3A)	7866	2987	8102	63
H(1A)	3875	5701	7310	46
H(2A)	5476	5548	9051	46
H(2B)	6988	5169	8090	46
H(3B)	6356	3556	9764	47
H(4A)	3778	2282	8695	45
H(4B)	3336	3331	9702	45
H(6A)	-602	4752	6692	61
H(6B)	1266	4687	6012	61
H(6C)	938	5729	7033	61
H(8A)	3949	2457	4227	74
H(8B)	5959	2703	4621	74
H(8C)	4829	3817	4021	74

Table S8. Torsion angles [°] for Ac-hyp-OMe.

C(5)-N(1)-C(1)-C(7)	-84.4(3)
C(4)-N(1)-C(1)-C(7)	97.2(2)
C(5)-N(1)-C(1)-C(2)	154.4(2)
C(4)-N(1)-C(1)-C(2)	-24.0(2)
N(1)-C(1)-C(2)-C(3)	37.7(2)
C(7)-C(1)-C(2)-C(3)	-84.7(2)
C(1)-C(2)-C(3)-O(3)	76.6(2)
C(1)-C(2)-C(3)-C(4)	-38.2(2)
C(5)-N(1)-C(4)-C(3)	-178.1(2)
C(1)-N(1)-C(4)-C(3)	0.3(3)
O(3)-C(3)-C(4)-N(1)	-92.8(2)
C(2)-C(3)-C(4)-N(1)	23.6(2)
C(1)-N(1)-C(5)-O(4)	180.0(2)
C(4)-N(1)-C(5)-O(4)	-1.9(4)
C(1)-N(1)-C(5)-C(6)	-0.1(4)
C(4)-N(1)-C(5)-C(6)	178.0(2)
C(8)-O(1)-C(7)-O(2)	-1.4(3)
C(8)-O(1)-C(7)-C(1)	174.5(2)
N(1)-C(1)-C(7)-O(2)	-165.6(2)
C(2)-C(1)-C(7)-O(2)	-50.3(3)
N(1)-C(1)-C(7)-O(1)	18.5(3)
C(2)-C(1)-C(7)-O(1)	133.8(2)

Table S9. Crystal Data and Structure Refinement for Crystalline Boc-mop-OH (**8**).

Identification code	raines09	
Empirical formula	$C_{11}H_{19}NO_5$	
Formula weight	245.27	
Temperature	105(2) K	
Wavelength	0.71073 Å	
Crystal system	Monoclinic	
Space group	$P2_1$	
Unit cell dimensions	a = 6.3770(16) Å	α = 90°
	b = 9.552(2) Å	β = 90.190(3)°
	c = 10.158(3) Å	γ = 90°
Volume	618.8(3) Å	
Z	2	
Density (calculated)	1.316 Mg/m^3	
Absorption coefficient	0.104 mm^{-1}	
F(000)	264	
Crystal size	0.52 × 0.36 × 0.10 mm^3	
Theta range for data collection	2.00 to 29.02°	
Index ranges	$-8 \le h \le 8$, $-12 \le k \le 13$, $-13 \le l \le 13$	
Reflections collected	10263	
Independent reflections	1727 [R_{int} = 0.0319]	
Completeness to theta = 29.02°	98.9%	
Absorption correction	Empirical with SADABS	
Max. and min. transmission	0.9897 and 0.9481	
Refinement method	Full-matrix least-squares on F^2	
Data / restraints / parameters	1727 / 1 / 160	
Goodness-of-fit on F^2	1.108	
Final R indices [$I > 2\sigma(I)$]	$R1$ = 0.0304, $wR2$ = 0.0767	
R indices (all data)	$R1$ = 0.0312, $wR2$ = 0.0771	
Absolute structure parameter	N/A	
Twin component ratio	0.6859(17):0.3141(17)	
Largest diff. peak and hole	0.228 and –0.124 e.$Å^{-3}$	

Table S10. Atomic Coordinates (10^4) and Equivalent Isotropic Displacement Parameters ($Å^2 \times 10^3$) for Boc-mop-OH (**8**).

	x	*y*	*z*	*U*(eq)[a]
O(1)	4942(2)	2938(2)	7524(2)	19(1)
O(2)	6991(3)	1640(2)	8923(2)	19(1)
O(3)	11034(2)	2033(2)	7257(2)	20(1)
O(4)	12392(2)	-100(2)	6901(2)	21(1)
O(5)	9609(3)	1045(2)	4325(2)	19(1)
N(1)	7097(3)	1241(2)	6778(2)	16(1)
C(1)	8634(3)	134(2)	6960(2)	15(1)
C(2)	8237(4)	-786(2)	5753(2)	19(1)
C(3)	7754(3)	307(2)	4690(2)	18(1)
C(4)	6376(3)	1358(2)	5397(2)	18(1)
C(5)	6260(3)	2018(2)	7731(2)	16(1)
C(6)	6784(4)	2581(2)	10070(2)	18(1)
C(7)	7881(4)	3955(3)	9775(2)	26(1)
C(8)	4496(4)	2788(3)	10445(3)	30(1)
C(9)	7954(5)	1775(3)	11144(2)	28(1)
C(10)	10898(3)	674(2)	7011(2)	15(1)
C(11)	11055(4)	226(3)	3600(2)	23(1)

[a] *U*(eq) is defined as one-third of the trace of the orthogonalized U^{ij} tensor.

Table S11. Bond lengths [Å] and angles [°] for Boc-mop-OH (**8**).

O(1)-C(5)	1.234(3)	C(3)-H(3A)	1.0000
O(2)-C(5)	1.346(3)	C(4)-H(4A)	0.9900
O(2)-C(6)	1.477(3)	C(4)-H(4B)	0.9900
O(3)-C(10)	1.324(3)	C(6)-C(7)	1.517(3)
O(3)-H(3)	0.8400	C(6)-C(8)	1.522(3)
O(4)-C(10)	1.211(3)	C(6)-C(9)	1.528(3)
O(5)-C(11)	1.418(3)	C(7)-H(7A)	0.9800
O(5)-C(3)	1.427(3)	C(7)-H(7B)	0.9800
N(1)-C(5)	1.333(3)	C(7)-H(7C)	0.9800
N(1)-C(1)	1.453(3)	C(8)-H(8A)	0.9800
N(1)-C(4)	1.478(3)	C(8)-H(8B)	0.9800
C(1)-C(2)	1.529(3)	C(8)-H(8C)	0.9800
C(1)-C(10)	1.534(3)	C(9)-H(9A)	0.9800
C(1)-H(1)	1.0000	C(9)-H(9B)	0.9800
C(2)-C(3)	1.533(3)	C(9)-H(9C)	0.9800
C(2)-H(2A)	0.9900	C(11)-H(11A)	0.9800
C(2)-H(2B)	0.9900	C(11)-H(11B)	0.9800
C(3)-C(4)	1.517(3)	C(11)-H(11C)	0.9800
C(5)-O(2)-C(6)	121.02(16)	O(2)-C(6)-C(9)	102.24(17)
C(10)-O(3)-H(3)	109.5	C(7)-C(6)-C(9)	110.6(2)
C(11)-O(5)-C(3)	113.75(17)	C(8)-C(6)-C(9)	110.7(2)
C(5)-N(1)-C(1)	125.75(17)	C(6)-C(7)-H(7A)	109.5
C(5)-N(1)-C(4)	121.51(18)	C(6)-C(7)-H(7B)	109.5
C(1)-N(1)-C(4)	112.55(16)	H(7A)-C(7)-H(7B)	109.5
N(1)-C(1)-C(2)	101.92(16)	C(6)-C(7)-H(7C)	109.5
N(1)-C(1)-C(10)	113.21(16)	H(7A)-C(7)-H(7C)	109.5
C(2)-C(1)-C(10)	111.95(17)	H(7B)-C(7)-H(7C)	109.5
N(1)-C(1)-H(1)	109.8	C(6)-C(8)-H(8A)	109.5
C(2)-C(1)-H(1)	109.8	C(6)-C(8)-H(8B)	109.5
C(10)-C(1)-H(1)	109.8	H(8A)-C(8)-H(8B)	109.5
C(1)-C(2)-C(3)	101.86(16)	C(6)-C(8)-H(8C)	109.5
C(1)-C(2)-H(2A)	111.4	H(8A)-C(8)-H(8C)	109.5
C(3)-C(2)-H(2A)	111.4	H(8B)-C(8)-H(8C)	109.5
C(1)-C(2)-H(2B)	111.4	C(6)-C(9)-H(9A)	109.5
C(3)-C(2)-H(2B)	111.4	C(6)-C(9)-H(9B)	109.5
H(2A)-C(2)-H(2B)	109.3	H(9A)-C(9)-H(9B)	109.5
O(5)-C(3)-C(4)	106.11(17)	C(6)-C(9)-H(9C)	109.5
O(5)-C(3)-C(2)	110.81(17)	H(9A)-C(9)-H(9C)	109.5
C(4)-C(3)-C(2)	103.41(17)	H(9B)-C(9)-H(9C)	109.5
O(5)-C(3)-H(3A)	112.0	O(4)-C(10)-O(3)	124.38(19)
C(4)-C(3)-H(3A)	112.0	O(4)-C(10)-C(1)	122.14(18)
C(2)-C(3)-H(3A)	112.0	O(3)-C(10)-C(1)	113.37(17)
N(1)-C(4)-C(3)	102.75(17)	O(5)-C(11)-H(11A)	109.5
N(1)-C(4)-H(4A)	111.2	O(5)-C(11)-H(11B)	109.5
C(3)-C(4)-H(4A)	111.2	H(11A)-C(11)-H(11B)	109.5
N(1)-C(4)-H(4B)	111.2	O(5)-C(11)-H(11C)	109.5
C(3)-C(4)-H(4B)	111.2	H(11A)-C(11)-H(11C)	109.5
H(4A)-C(4)-H(4B)	109.1	H(11B)-C(11)-H(11C)	109.5
O(1)-C(5)-N(1)	123.20(19)		
O(1)-C(5)-O(2)	125.29(19)		
N(1)-C(5)-O(2)	111.49(18)		
O(2)-C(6)-C(7)	109.14(17)		
O(2)-C(6)-C(8)	111.39(19)		
C(7)-C(6)-C(8)	112.3(2)		

Table S12. Anisotropic Displacement Parameters ($Å^2 \times 10^3$) for Boc-mop-OH (**8**).[a]

	U^{11}	U^{22}	U^{33}	U^{23}	U^{13}	U^{12}
O(1)	16(1)	16(1)	24(1)	-1(1)	-2(1)	1(1)
O(2)	22(1)	18(1)	18(1)	-2(1)	0(1)	4(1)
O(3)	14(1)	16(1)	30(1)	-4(1)	-1(1)	1(1)
O(4)	18(1)	18(1)	26(1)	2(1)	3(1)	4(1)
O(5)	22(1)	16(1)	19(1)	0(1)	2(1)	-2(1)
N(1)	13(1)	17(1)	18(1)	-1(1)	-2(1)	0(1)
C(1)	18(1)	12(1)	15(1)	1(1)	2(1)	0(1)
C(2)	23(1)	12(1)	21(1)	-1(1)	1(1)	-2(1)
C(3)	21(1)	16(1)	18(1)	-2(1)	-2(1)	-2(1)
C(4)	18(1)	22(1)	15(1)	-2(1)	-2(1)	1(1)
C(5)	13(1)	16(1)	20(1)	-2(1)	2(1)	-4(1)
C(6)	22(1)	16(1)	16(1)	-1(1)	3(1)	1(1)
C(7)	37(1)	21(1)	21(1)	-1(1)	-1(1)	-8(1)
C(8)	26(1)	32(1)	32(1)	0(1)	12(1)	6(1)
C(9)	39(1)	26(1)	19(1)	1(1)	-2(1)	7(1)
C(10)	17(1)	16(1)	12(1)	2(1)	-2(1)	0(1)
C(11)	26(1)	23(1)	21(1)	-1(1)	4(1)	1(1)

[a]The anisotropic displacement factor exponent takes the form: $-2p^2[h^2 a^{*2}U^{11} + ... + 2\ h\ k\ a^*\ b^*\ U^{12}]$

.

Table S13. Hydrogen Coordinates ($\times 10^4$) and Isotropic Displacement Parameters ($Å^2 \times 10^3$) for Boc-mop-OH (**8**).

	x	*y*	*z*	*U*(eq)
H(3)	12301	2265	7313	24
H(1)	8313	-402	7780	18
H(2A)	7033	-1423	5893	22
H(2B)	9492	-1346	5527	22
H(3A)	7029	-115	3910	22
H(4A)	6595	2316	5053	22
H(4B)	4875	1110	5313	22
H(7A)	7189	4414	9028	39
H(7B)	9352	3772	9557	39
H(7C)	7811	4564	10549	39
H(8A)	3776	1881	10441	45
H(8B)	3821	3415	9808	45
H(8C)	4417	3200	11327	45
H(9A)	9392	1589	10856	42
H(9B)	7236	886	11312	42
H(9C)	7984	2333	11953	42
H(11A)	10317	-258	2884	35
H(11B)	11707	-466	4184	35
H(11C)	12142	834	3230	35

Table S14. Torsion Angles [°] for Boc-mop-OH (**8**).

C(5)-N(1)-C(1)-C(2)	154.43(19)
C(4)-N(1)-C(1)-C(2)	-20.6(2)
C(5)-N(1)-C(1)-C(10)	-85.2(2)
C(4)-N(1)-C(1)-C(10)	99.8(2)
N(1)-C(1)-C(2)-C(3)	37.32(19)
C(10)-C(1)-C(2)-C(3)	-84.0(2)
C(11)-O(5)-C(3)-C(4)	-177.70(18)
C(11)-O(5)-C(3)-C(2)	70.7(2)
C(1)-C(2)-C(3)-O(5)	71.9(2)
C(1)-C(2)-C(3)-C(4)	-41.4(2)
C(5)-N(1)-C(4)-C(3)	179.68(18)
C(1)-N(1)-C(4)-C(3)	-5.1(2)
O(5)-C(3)-C(4)-N(1)	-88.01(19)
C(2)-C(3)-C(4)-N(1)	28.7(2)
C(1)-N(1)-C(5)-O(1)	-179.29(19)
C(4)-N(1)-C(5)-O(1)	-4.7(3)
C(1)-N(1)-C(5)-O(2)	-1.0(3)
C(4)-N(1)-C(5)-O(2)	173.58(18)
C(6)-O(2)-C(5)-O(1)	-19.5(3)
C(6)-O(2)-C(5)-N(1)	162.30(18)
C(5)-O(2)-C(6)-C(7)	-58.8(2)
C(5)-O(2)-C(6)-C(8)	65.8(3)
C(5)-O(2)-C(6)-C(9)	-175.96(19)
N(1)-C(1)-C(10)-O(4)	-165.41(18)
C(2)-C(1)-C(10)-O(4)	-50.9(3)
N(1)-C(1)-C(10)-O(3)	18.2(2)
C(2)-C(1)-C(10)-O(3)	132.72(18)

400 MHz ^{1}H NMR Spectrum of Compound **2**

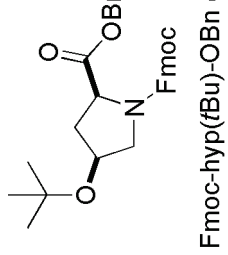

Fmoc-hyp(*t*Bu)-OBn (**2**)

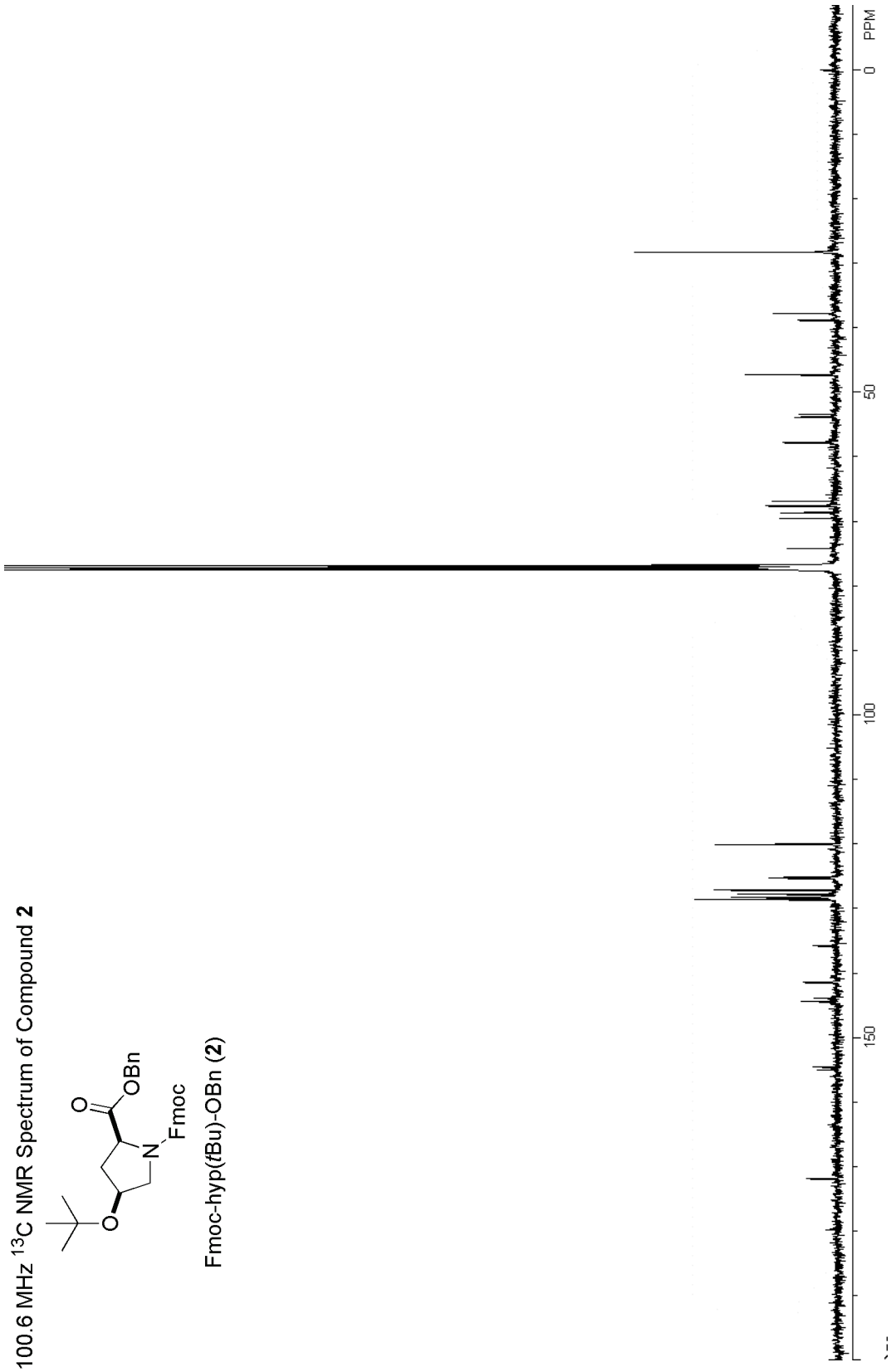
100.6 MHz ^{13}C NMR Spectrum of Compound **2**
Fmoc-hyp(*t*Bu)-OBn (**2**)
O
OBn
N
Fmoc
O
O
PPM
0
50
100
150

400 MHz ^{1}H NMR Spectrum of Compound **3**

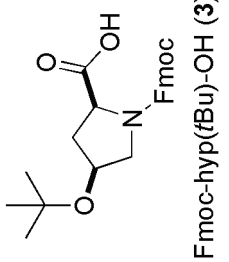

Fmoc-hyp(*t*Bu)-OH (**3**)

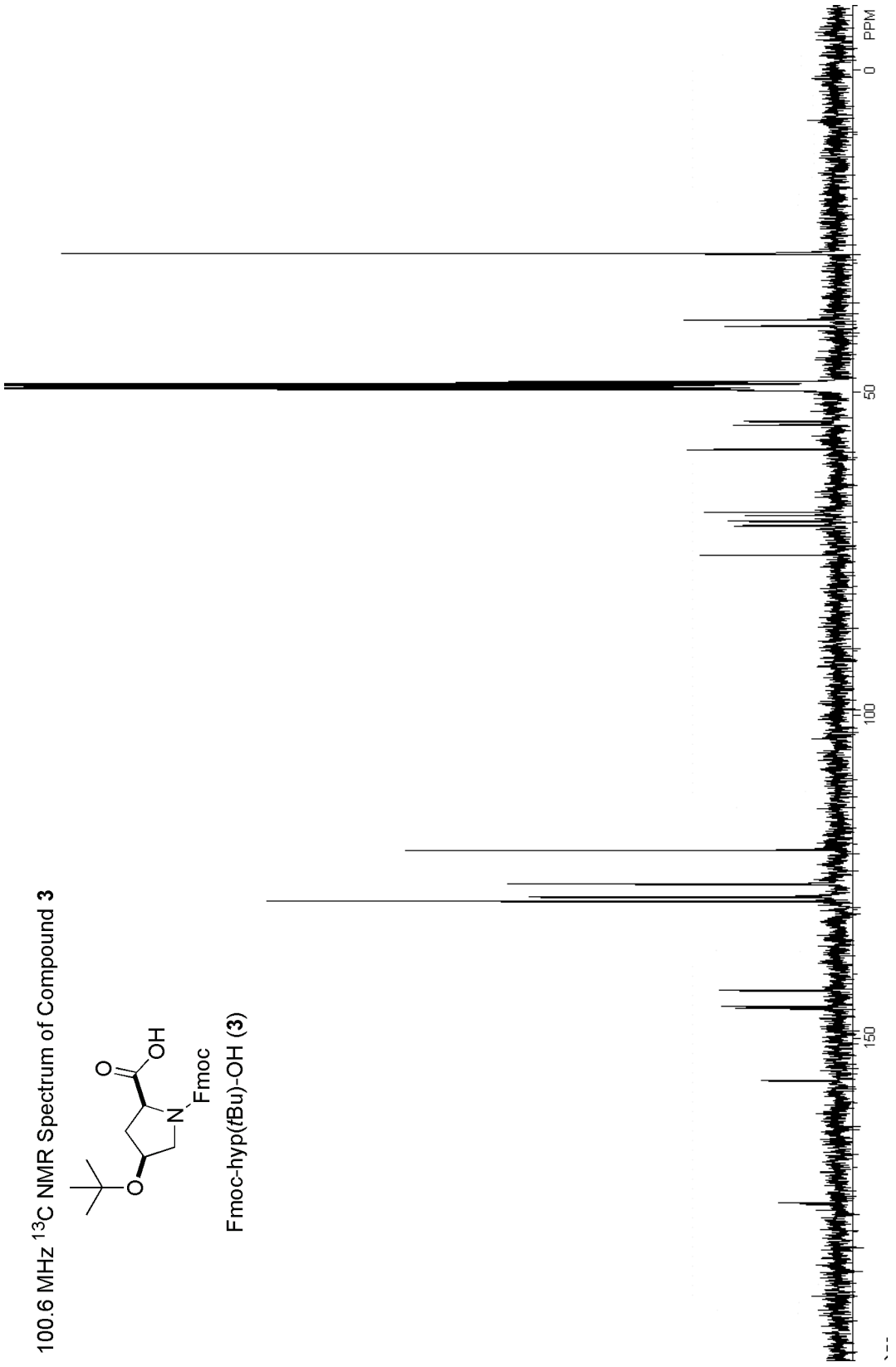
100.6 MHz ^{13}C NMR Spectrum of Compound **3**
Fmoc-hyp(*t*Bu)-OH (**3**)
Fmoc
OH
O
O
N
PPM
0
50
100
150

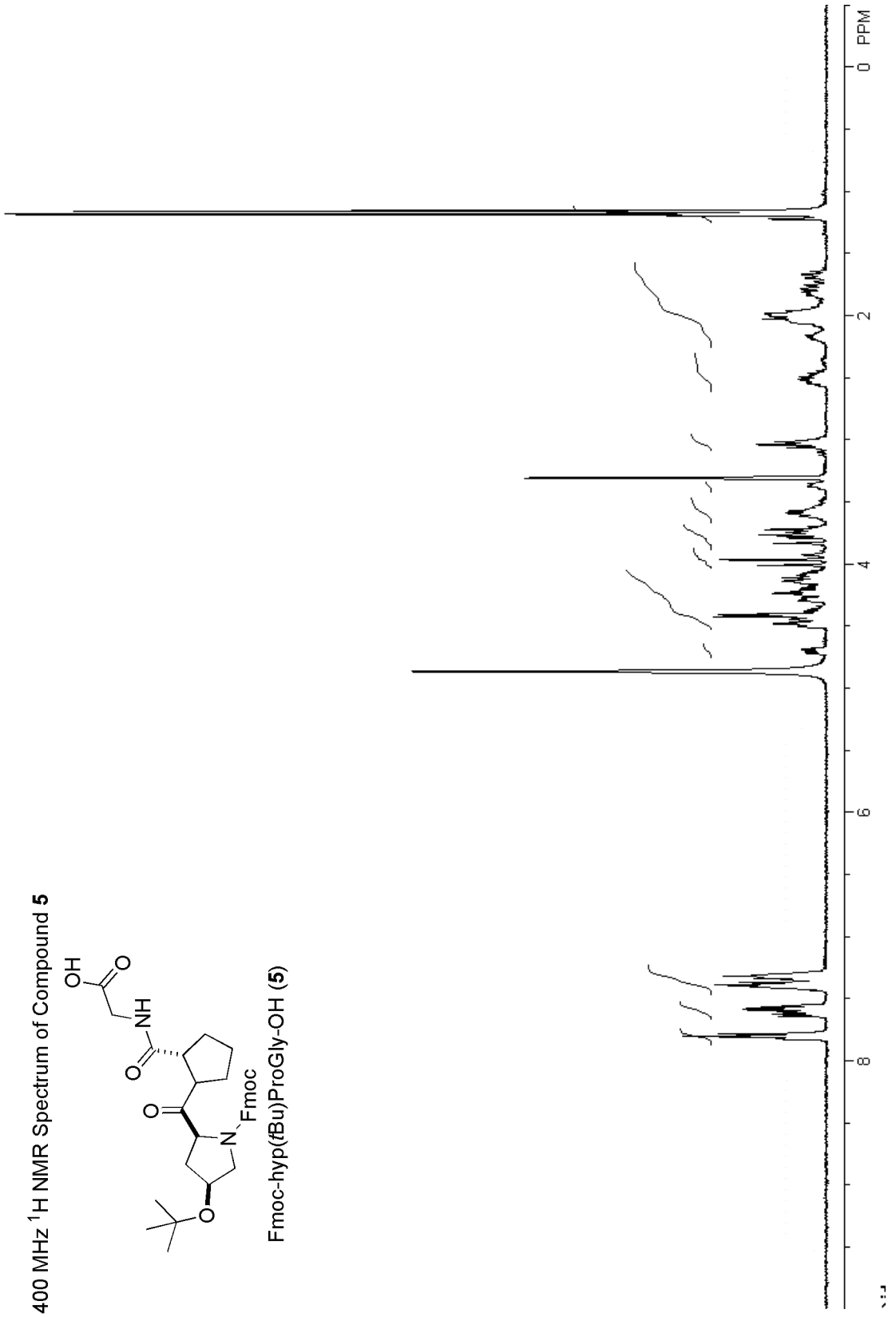
400 MHz ^{1}H NMR Spectrum of Compound **5**
Fmoc-hyp(*t*Bu)ProGly-OH (**5**)
OH
O
NH
O
O
N
Fmoc
O
8
6
4
2
0 PPM

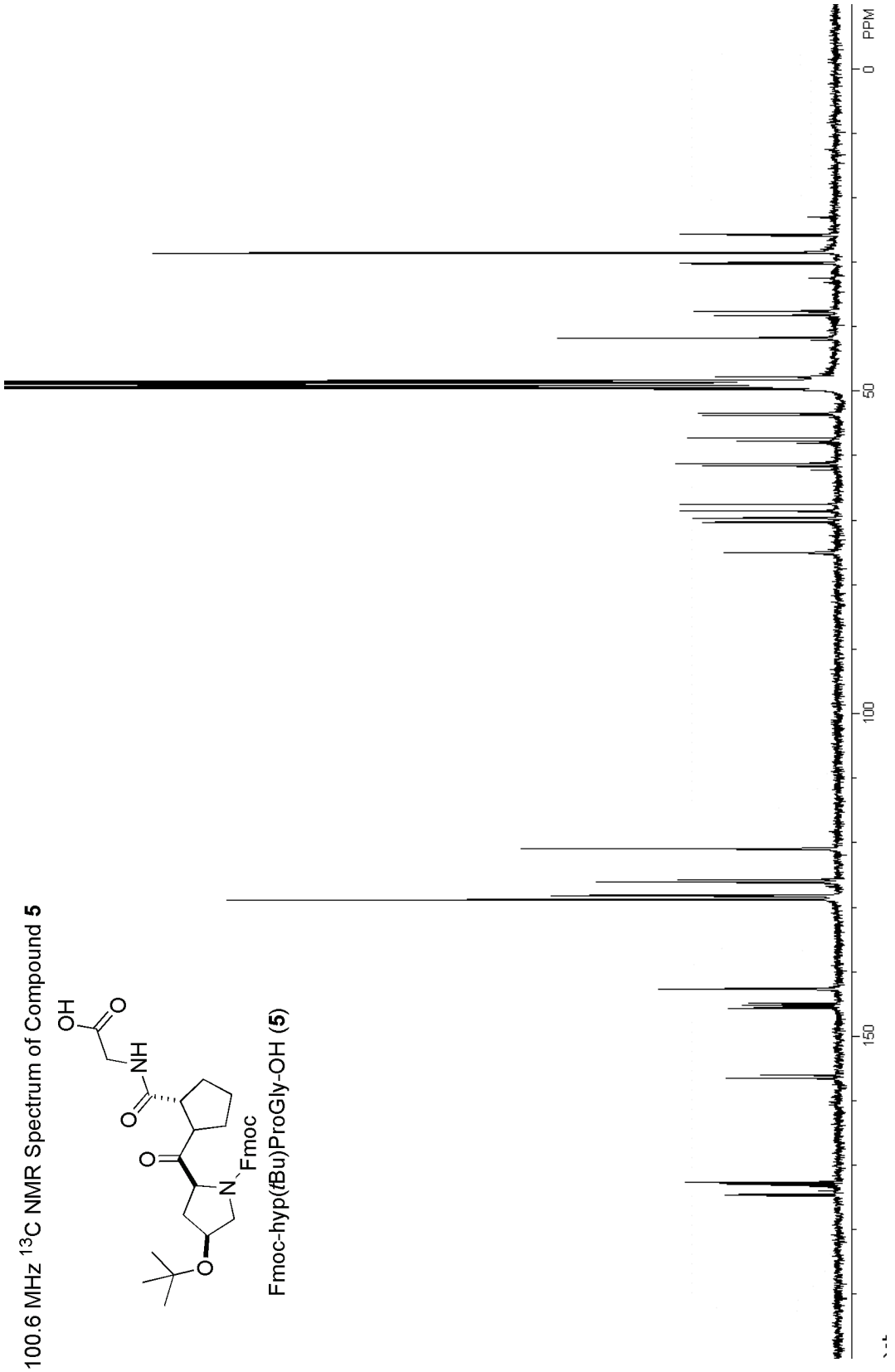
100.6 MHz ^{13}C NMR Spectrum of Compound **5**
Fmoc-hyp(*t*Bu)ProGly-OH (**5**)
OH
O
NH
O
O
N
Fmoc
O
PPM
0
50
100
150

400 MHz ^{1}H NMR Spectrum of Compound **7**

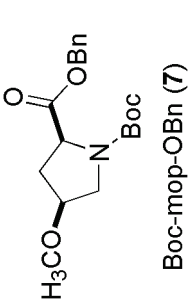

Boc-mop-OBn (**7**)

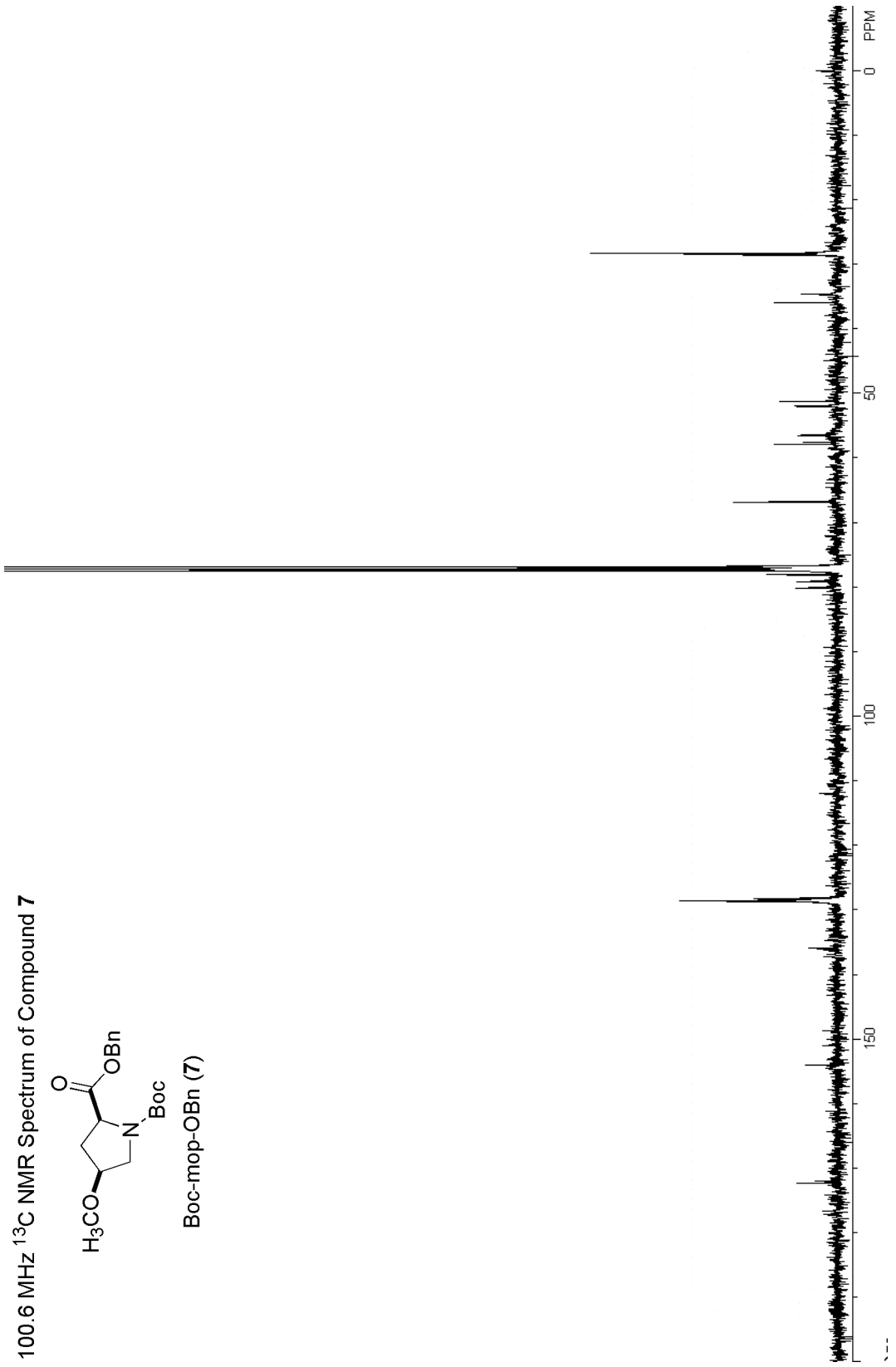
100.6 MHz ^{13}C NMR Spectrum of Compound **7**
O
OBn
N
Boc
H_3CO
Boc-mop-OBn (**7**)
PPM
0
50
100
150

400 MHz ^{1}H NMR Spectrum of Compound **8**

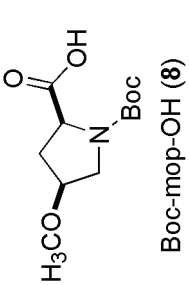

Boc-mop-OH (**8**)

100.6 MHz ^{13}C NMR Spectrum of Compound **8**

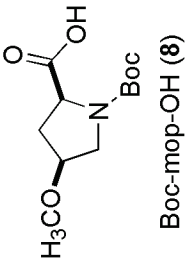

Boc-mop-OH (**8**)

400 MHz ^{1}H NMR Spectrum of Compound **9**

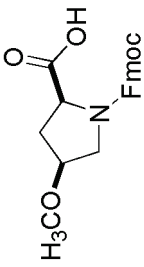

Fmoc-mop-OH (**9**)

100.6 MHz ^{13}C NMR Spectrum of Compound **9**

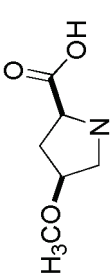

Fmoc-mop-OH (**9**)

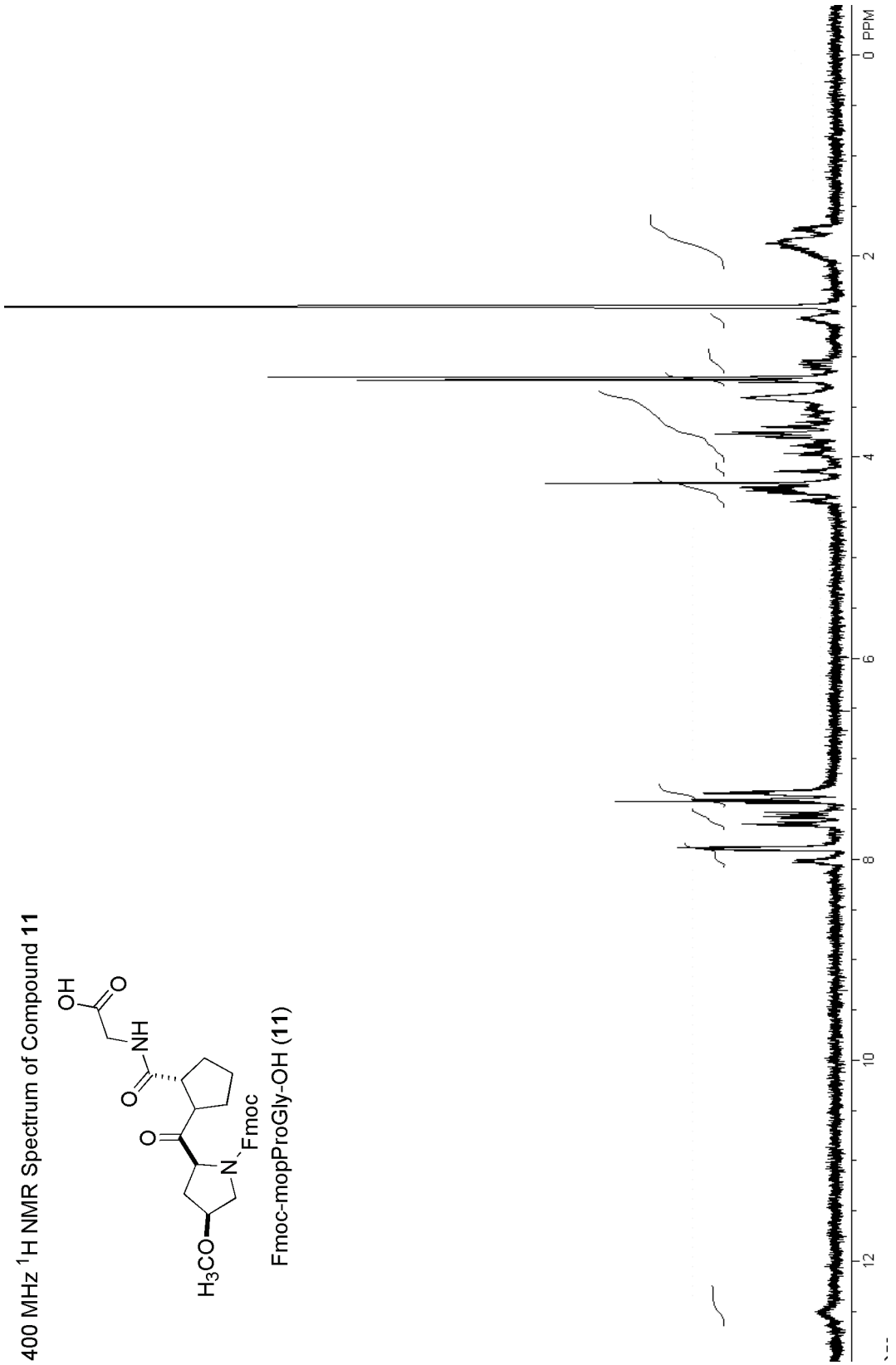
400 MHz ^{1}H NMR Spectrum of Compound **11**
Fmoc-mopProGly-OH (**11**)
OH
O
NH
O
O
N
Fmoc
H_3CO
0
2
4
6
8
10
12
PPM

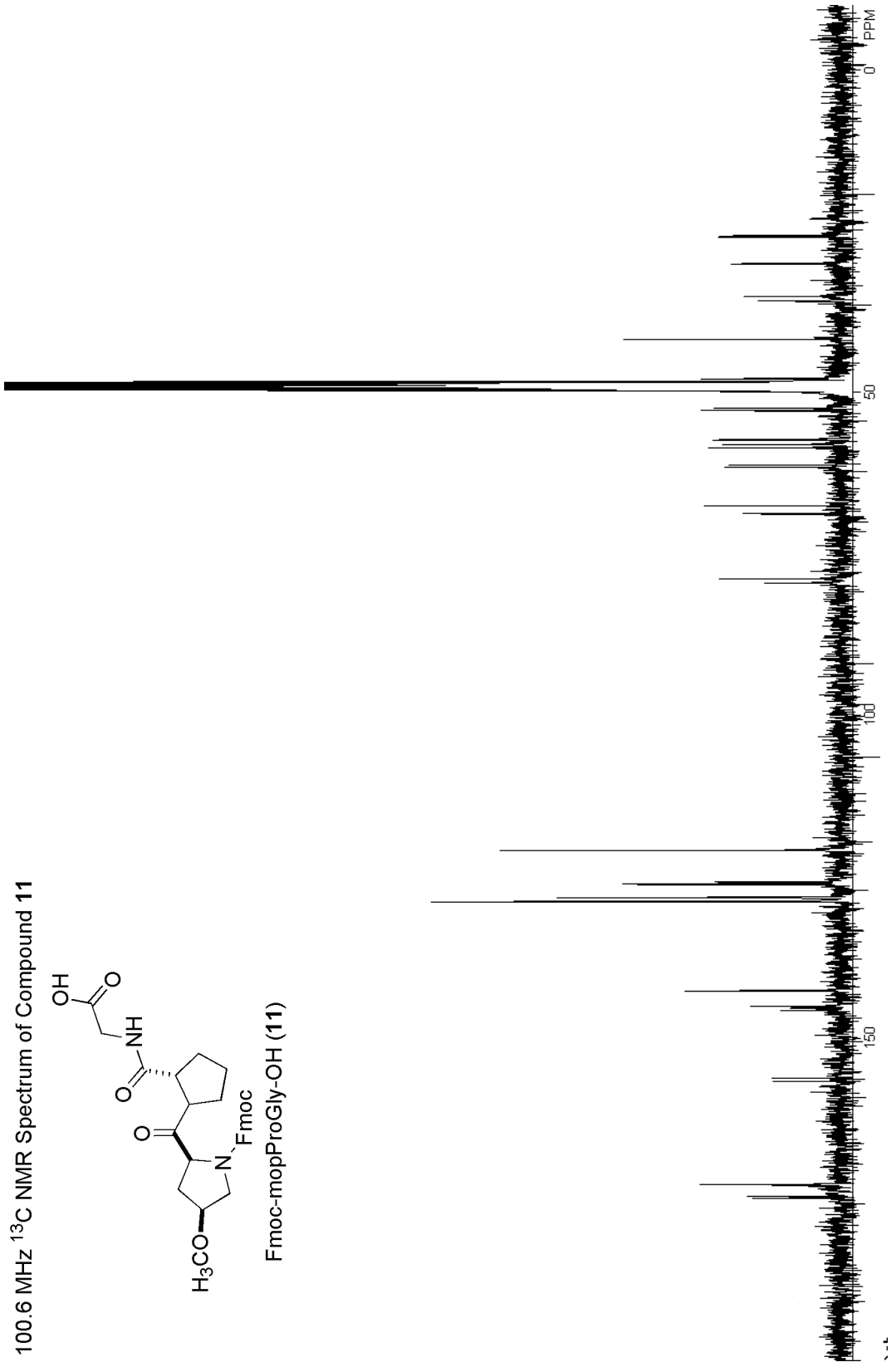
100.6 MHz ^{13}C NMR Spectrum of Compound **11**
Fmoc-mopProGly-OH (**11**)
OH
O
NH
O
O
N
Fmoc
H_3CO
PPM
0
50
100
150

400 MHz ^{1}H NMR Spectrum of Ac-mop-OMe

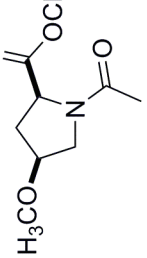

Ac-mop-OMe

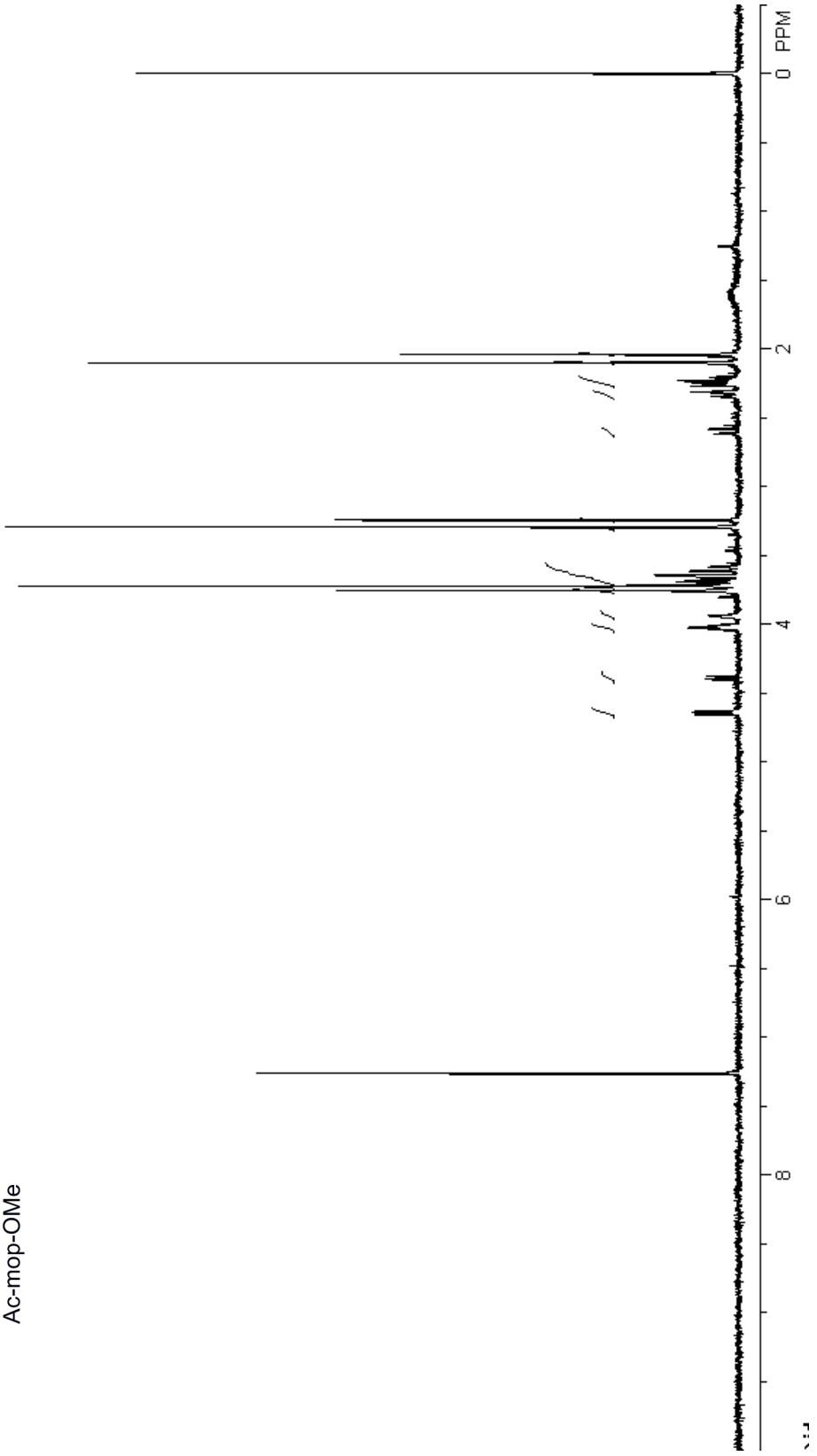

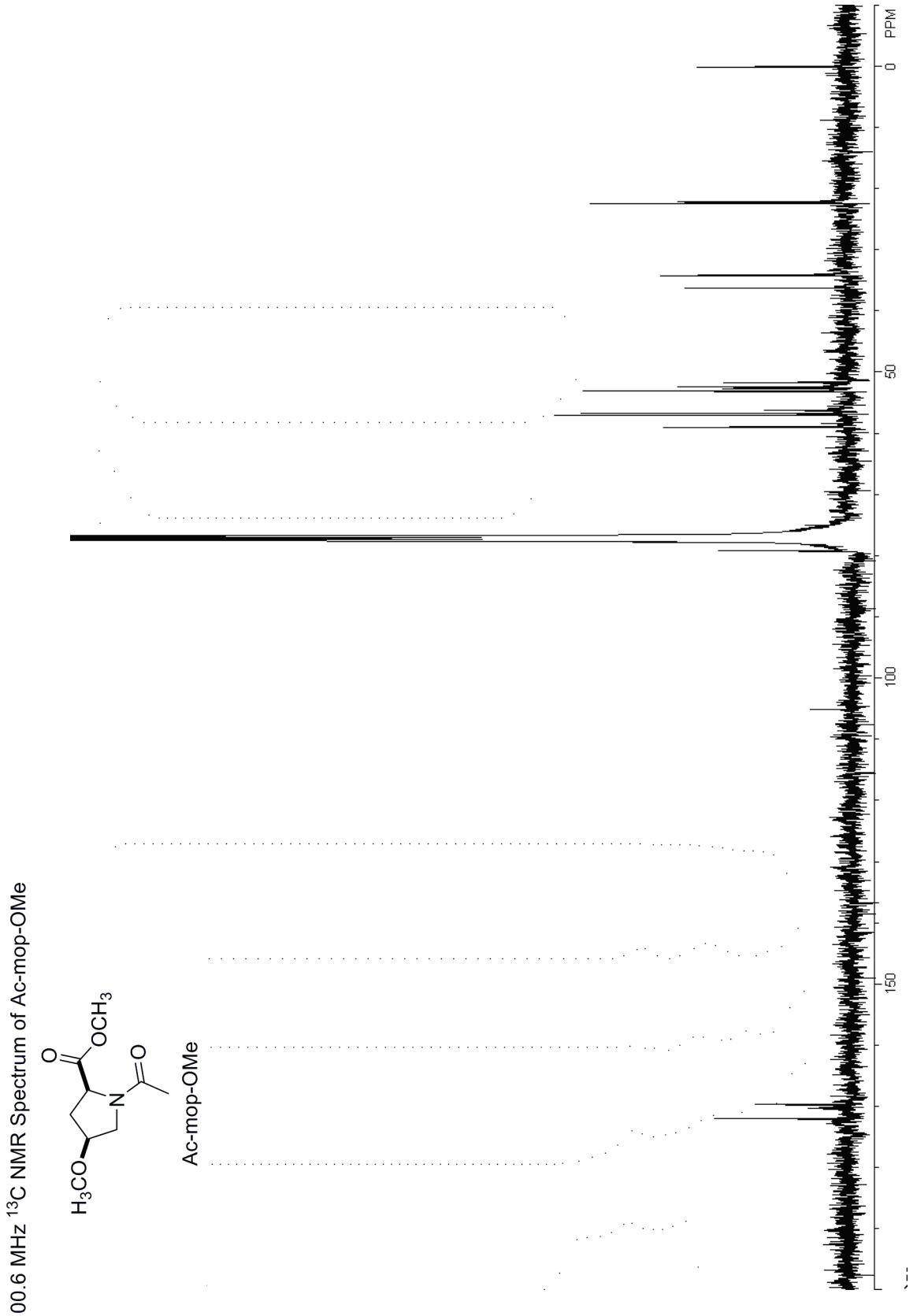
100.6 MHz ^{13}C NMR Spectrum of Ac-mop-OMe
Ac-mop-OMe
PPM
0
50
100
150